Vector-meson reconstruction in the ePIC backward HCal

Vincent Andrieux, Roland Nothnagel, Caroline Riedl, Dhruv Sharma

University of Illinois Urbana-Champaign

Version 1.0

November 22, 2024

Abstract

This document summarizes simulation studies of diffractive vector-meson production at ePIC and the reconstruction of the decay particles in the ePIC backward HCal (nHCal) and the other hadronic calorimeters.

Contents

1 Diffractive vector-meson production and the ePIC nHCal

One important physics pillar of ePIC (Fig. 1.1), the day-1 detector at the electron-ion collider (EIC), is the exploration of nucleon and nucleus tomography in position space,

hadronic calorimeter	η_{min}	η_{max}
nHCal	-4.05	-1.20
barrel	-1.20	+1.18
LFHCal	+1.18	+4.2

Table 1.1: Used acceptances in pseudo-rapidity η (as defined in Fig. 1.2) for the three ePIC hadronic calorimeters in the backward endcap (nHCal), the barrel, and the forward endcap (LFHCal). Note that the acceptances are defined to be not overlapping.

i.e., are the quarks and gluons located rather at the edge, or in the periphery of the probed hadron? How does this picture change with varying parton longitudinal momenta and other kinematic parameters? This information is encoded in Generalized Parton Distributions (GPDs) [1].

In deep-inelastic lepton-hadron scattering (DIS), in general ℓH$\rightarrow \ell$X, and ep/A$\rightarrow$eX at the EIC, the proton p or nucleus A does not break up in about 10% of the cases; this is referred to as diffractive DIS, or DDIS [2]. Such types of events were found in ep by the HERA collaborations[1] to have the typical large rapidity gap, i.e., a wide range in rapidity (see Fig. 1.2) without activity in the detectors. In some of these diffractive events, a vector meson (VM) is produced without other activity in the event, carrying information about hadron structure. This case is referred to as exclusive VM production, as shown in Fig. 1.3 [3]. One also distinguishes between "no proton excitation" (coherent, as in Fig. 1.3) and "proton excitation" (incoherent). Exclusive vector-meson production in DDIS will be a powerful tool at the EIC to explore the multidimensional structure of hadrons.

In this document, we will investigate how many decay products from diffractively produced VMs at the EIC end up in the acceptance of the ePIC nHCal and the other hadronic calorimeters, as sketched in Fig. 1.1. We used the acceptance boundaries in pseudo-rapidity as listed in Tab. 1.1. We looked at standalone simulations and centrally produced productions including the full ePIC geometry and reconstruction. In Sec. 2, we describe our particle/track-based analysis. We summarize and give an outlook to future studies in Sec. 3. Appendix A compiles some basic information about the centrally produced ePIC simulations and their analysis.

2 Particle and track level

2.1 Central productions 101

Following the analysis steps detailed in App. A, centrally produced ePIC simulation samples were analyzed (Caroline, CR [4]) for VM decays and the occurrence of VM decay products in the rapidity acceptance of the nHCal. For the time being, these studies used already existing simulation productions. Vector mesons and their decay products were identified on generator level. It was then checked whether the decay products were reconstructed. The results from `pythia` data `EPIC/RECO/24.07.0/epic_craterlake/DIS/NC/18x275/minQ2=1` for $\rho^0 \rightarrow \pi^+\pi^-$ and $\phi \rightarrow K^+K^-$ decays are shown in Fig. 2.1. About 4% of the reconstructed decay pions and about 6% of the reconstructed decay kaons are in the pseudo-rapidity acceptance of the nHCal. As expected, higher Q^2 values ($1 \rightarrow 1000$ GeV^2) reduce the fraction of decay mesons in the nHCal. A generic DIS sample as generated by `pythia` suffers for

[1] H1 and ZEUS at the HERA ep-collider at DESY, Germany

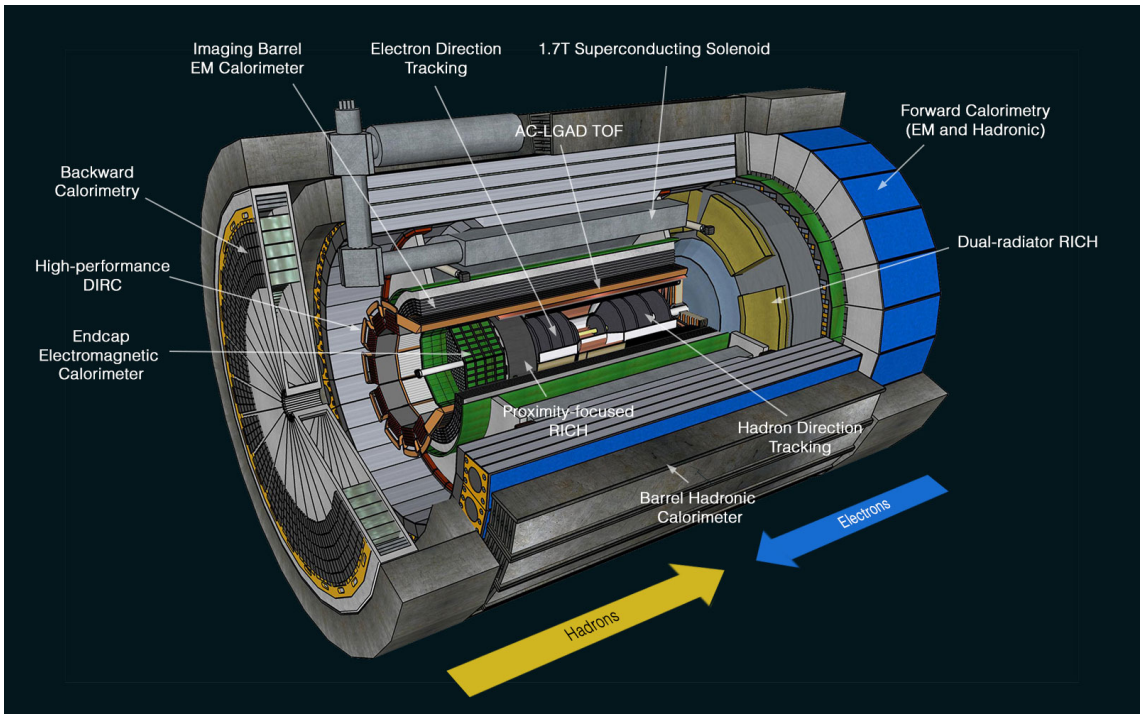

Figure 1.1: Rendering of the ePIC detector with barrel and endcaps, cut open to show the inner layers. Hadrons (from the left) collide with electrons (from the right) in the center of the barrel. The backward / electron-going hadronic calorimeter, or nHCal, labeled "Backward Calorimetry" here, is the disk facing the left edge of the image.

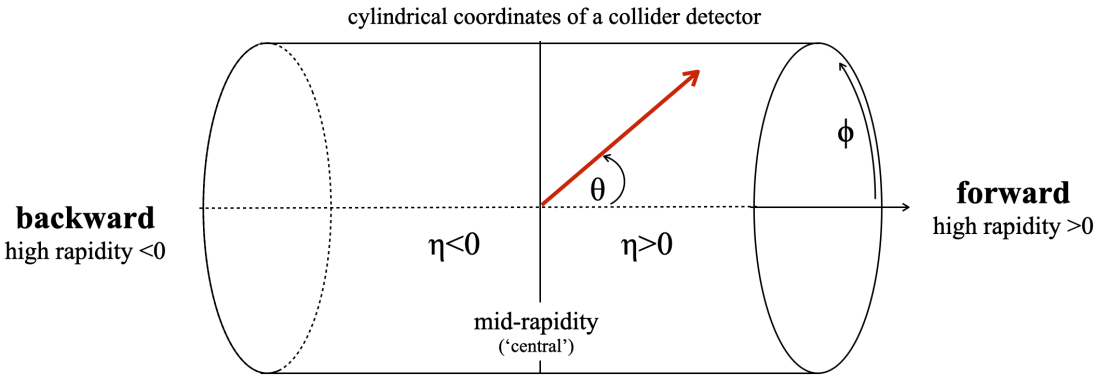

Figure 1.2: The cylindrical coordinate system with azimuthal and polar angles (ϕ, η) typically used for a collider detector. Since we are dealing with a highly relativistic system, we conveniently define rapidity as $y = 1/2 \cdot \ln \frac{1+\beta\cos\theta}{1+\beta\cos\theta}$. Since it is easier to measure and almost identical to y for highly relativistic particles, one defines (for particles with ≈ 0 mass) the pseudo-rapidity $\eta = -\ln\tan(\theta/2)$.

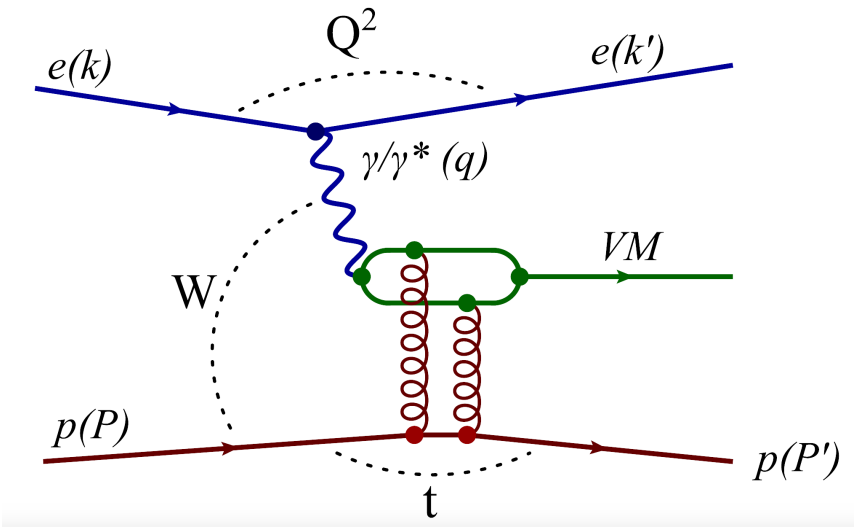

Figure 1.3: Exclusive vector meson production, a subcategory of diffractive DIS.

certain decays from low branching ratios (BR), making it CPU-expensive and impractical to study these decays. For example, ρ^0 decays to di-leptons have BR$\sim$ 0.00005, and in the `pythia` minQ2=1 sample, there are only 6 J/ψs for about 1M generated events.

In order to study dedicated processes and decays, it is often advisable to use dedicated event generators tailored for this purpose. Diffractively produced VMs were studied as generated by the `sartre` event generator in coherent production: eAu$\rightarrow$eAuϕ ($\rightarrow K^+K^-$) from `EPIC/RECO/24.07.0/epic_craterlake/EXCLUSIVE/DIFFRACTIVE_PHI_ABCONV/Sartre/Coherent`. The beam energies are (18x110), the used dipole model is `bNonSat`, the dipole model parameter set KMW, the kinematic limits are $t = [0.5, \sim 0]$; $Q^2 = [1, 20]$; $W = [1.95772, 88.9985]$, and the `sartre` release is 1.39. The sample consists of one generated and decaying ϕ-meson per event and there are plenty of events centrally generated and reconstructed. This is not the case for diffractively produced $J/\psi \rightarrow ee$ with `sartre`. Only generated events were found in `S3/eictest/EPIC/EVGEN/EXCLUSIVE/DIFFRACTIVE_JPSI_ABCONV/Sartre/Coherent` and there was no parallel `RECO` directory with reconstructed events. For a first feasibility study, 100 events were reconstructed using `npsim`. Figure 2.2 shows the results. About 42% of the ϕ decay kaons and about 55% of the J/ψ decay electrons are found to be in the η acceptance of the nHCal. A summary of the event generators and VM decays of CR's initial study is shown in Fig. 2.3.

2.2 Standalone event generator

In parallel to the studies with centrally produced simulation samples, diffractive VM decays were studied using samples generated with standalone `sartre` (Vincent, VA [5, 6]). These studies include a more detailed look at decay fractions in the nHCal including their kinematic dependence. The used `sartre` release was 1.33. Diffractively produced exclusive ρ^0, ϕ, and J/ψ meson decays at different beam energies and collision species were studied. Transverse momentum versus pseudo-rapidity distributions of VM decay products $ep \rightarrow ep$VM at beam energies (18x275) are shown in Fig. 2.4. Decay products from different VMs appear to be distributed differently in kinematic phase space, some more populating the backward region.

Next, it was counted how many decay products for a given VM decay ended up in

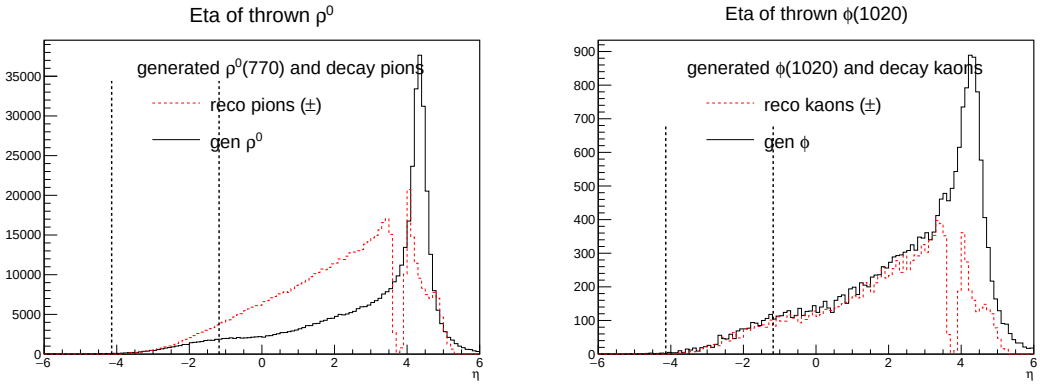

Figure 2.1: Pseudo-rapidity distributions of $\rho^0 \to \pi^+\pi^-$ (left) and $\phi \to K^+K^-$ (right) decays in about 1M generated events of `pythia` NC minQ2=1. The black histogram is the generated η of the mother VM; the red histogram the reconstructed η of the decay daughters. The rapidity range of the nHCal is indicated by the vertical dashed lines.

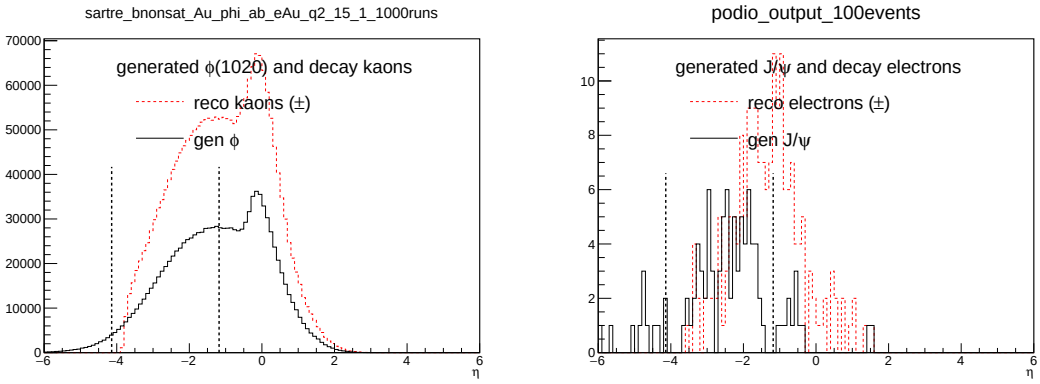

Figure 2.2: Pseudo-rapidity distributions of $\phi \to K^+K^-$ (left, 1.2M events) and $J/\psi \to e^+e^-$ (right, 100 events) decays in `sartre` (coherent). Otherwise as caption of Fig. 2.1.

percentage of **any reco decay particles** in nHCal acceptance	pythia8NCDIS_18x275_minQ2_1or10 DIS NC minQ2 1 or 10	pythia8NCDIS_18x275_minQ2_100 DIS NC minQ2 100	pythia8CCDIS_18x275_minQ2_100 DIS CC minQ2 100	pythia_ep_18x275_q2_0.000000001 Photoproduction (low Q2)	rho_10x100_uChannel_Q2of0to10_hiDiv rho u-channel	sartre_bnonsat_Au_phi_ab_eAu_q2_15_1 excl phi	sartre rho? excl rho?	sartre_bnonsat_Au_jpsi_ab_eAu excl J/Psi (reco by CKR with npsim)
$\rho \to \pi^+\pi^-$	4%	2%	2%	8%	No rho generated. Only see decay pions. not in nHCal	-	only EVGEN. reconstruct yourself	-
$\rho \to \mu^+\mu^-$	BR ~0.00005				^^	-		-
$\rho \to e^+e^-$					^^	-		-
$\phi \to K^+K^-$	6%	3%	2%	9%	-	42%	-	-
$\phi \to K^+K^- \to \mu^+\mu^-$	kaons are treated as stable particles (GenStatus==1) and are not decayed				-	kaons are not decayed	-	-
$J/\psi \to e^+e^-$	very few J/Psi generated && very low BR				-	-	-	54.5%
$J/\psi \to \mu^+\mu^-$					-	-	-	only decays to ee

Figure 2.3: Studied event generators and VM decays from the centrally produced simulation samples.

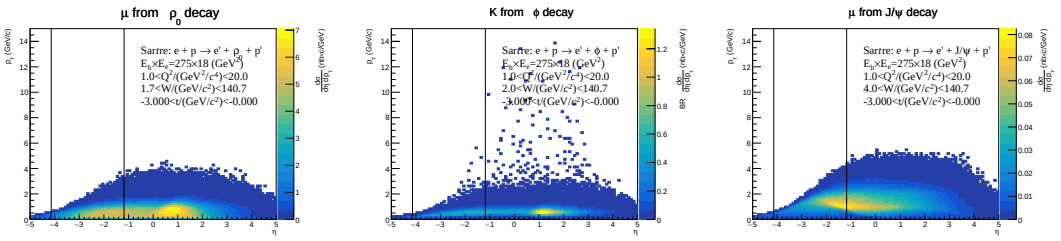

Figure 2.4: (η, p_T) distributions of decay products from `sartre` standalone diffractively produced ρ^0 (left), ϕ (middle), and J/ψ (right) mesons. The nHCal acceptance is indicated by the vertical solid lines.

the η-acceptance of which ePIC hadronic calorimeter, as given in Tab. 1.1. The resulting fractions for each possible combination are represented by the matrix tables in Figs. 2.5 (ep collisions) and 2.6 (eAu collisions) There is also an "any" HCal category for that the η-acceptances of all HCals are combined. The kinematic dependencies of 0, 1, or 2 decay products in the η-acceptance of the nHCal are also shown. There is a region at low x-Bjorken where the nHCal takes over from the other ePIC hadronic calorimeters. Similar statements can be made for x-Pomeron and t-Mandelstam. This will be discussed in greater detail in Sec. 2.3. As shown in Fig. 2.6, fractions of decay products in the nHCal are higher for the studied eAu (20x100) sample, as compared to ep (18x275) collisions.

2.3 Refined analysis of central productions

The UIUC undergraduate students Dhruv (DS) and Roland (RN) repeated the more detailed studies from Sec. 2.2 using centrally produced simulation samples [7]. Ten runs, corresponding to about 12k events, were analyzed from the diffractive ϕ `sartre` sample described in Sec. 2.1. The (x, Q^2)-distribution of this data sample is shown in Fig. 2.7. The η-distribution of the generated and reconstructed decay kaons, and the resulting fractions in all possible combinations of ePIC HCals are shown in Fig. 2.8. For most of the events, both kaons were either in the barrel HCal (~47%) or in the nHCal (~44%) acceptance.

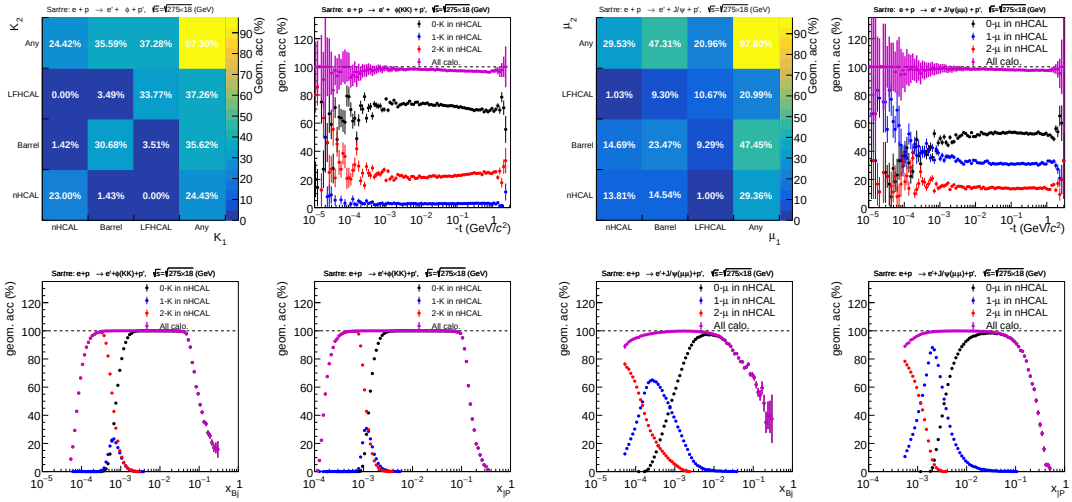

Figure 2.5: Fractions in an HCal acceptance of decay products for `sartre` standalone $\phi \to K_1K_2$ (set of left four panels) and $J/\psi \to \mu_1\mu_2$ (set of right four panels) diffractively produced in ep collisions (18x275). All combinations of ePIC HCals are investigated, as indicated by the matrix for the integrated kinematics. The other three panels show each the kinematic dependence (x_{Bj}, $x_{\mathbb{P}}$, t-Mandelstam) for the three cases of 0, 1, or 2 decay products in the nHCal. The fraction for (K_1, K_2) to be in any hadronic calorimeter is found to be 97.30% and that for (μ_1, μ_2) 97.80% (numbers in yellow boxes).

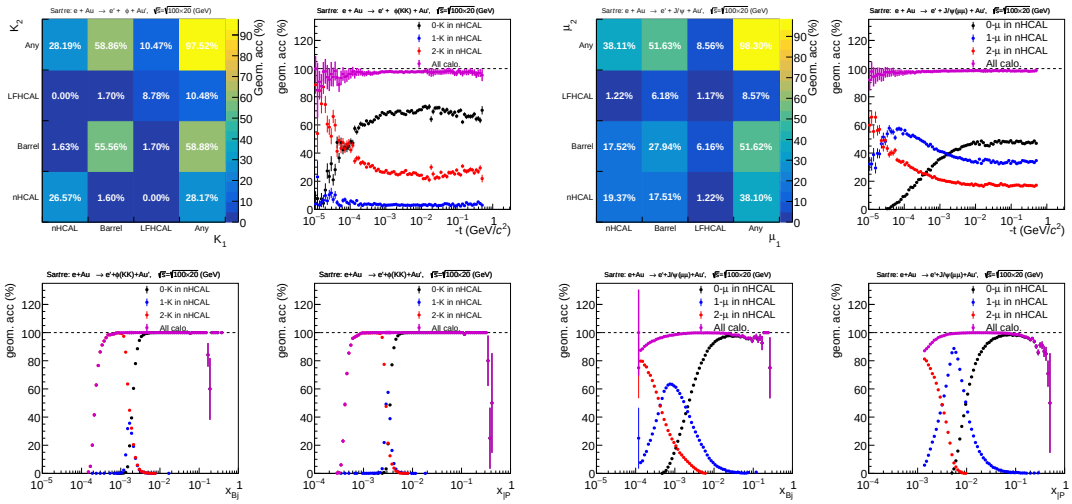

Figure 2.6: As caption of Fig. 2.5, but for eAu (20x100) collisions instead of ep (18x275). The fraction for (K_1, K_2) to be in any hadronic calorimeter is 97.52% and that for (μ_1, μ_2) is 98.30% (numbers in yellow boxes).

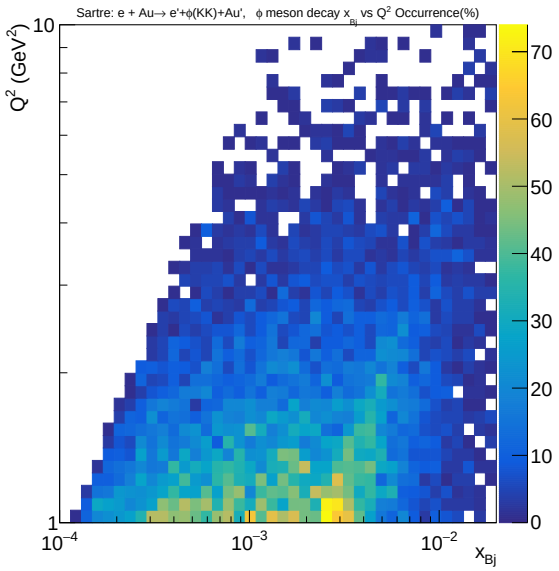

Figure 2.7: (x, Q^2)-distribution for `sartre` central production $\phi \to KK$ diffractively produced in eAu collisions (18x110).

Without the nHCal, about half of the ϕ decays would have incomplete, or no hadronic calorimeter information at all.

The fractions of 0, 1, or 2 reconstructed decay kaons in the nHCal acceptance are shown in Figure 2.9 together with how these categories are distributed in x-Bjorken. Events for that both (no) kaons are in the nHCal η-acceptance tend to populate lower (higher) x-Bjorken. For x-Bjorken between $3 \cdot 10^{-4}$ and $1.5 \cdot 10^{-3}$, one or two kaons end up in the nHCal η-acceptance. In agreement with the right hand side of Fig. 2.8, for almost all events for that both kaons were reconstructed by ePIC, the reconstructed kaons are in the η-acceptance of one of the ePIC HCals ("all calo").

The analysis was cross checked between DS and RN using independently developed `root` analysis macros and the identical set of simulated runs. Kinematic distributions were found to be matching and the fractional numbers in Fig. 2.8 to be in perfect agreement.

The results of this analysis agrees qualitatively with that in Sec. 2.2 in the sense that the nHCal is demonstrated to be important for decay products at low x-Bjorken. There are however some differences in the numbers comparing Fig. 2.6 top left (standalone `sartre`) and Fig. 2.8 right (centrally produced `sartre`). The slightly different beam energies [(18x110) for central, (20x100) for standalone] are not expected to play a major role. Secondly, the analyses differ with respect to generated and reconstructed level - the standalone looks at generated level only, while the central requires tracks to be reconstructed by ePIC. This could in addition to differing kinematic distributions cause differences in the normalization of the resulting fractions. The kinematic limits in Q^2, W and $-t$ used in the standalone production are comparable to that used for the central one. The used `sartre` releases are however different, and there may be possible subtleties in the used generator settings that do not match between the two productions. This is confirmed by a check (not shown) revealing that the η-distribution for the standalone `sartre` with (18x110) is sparser populated at lower η than the central production. Further checks are ongoing.

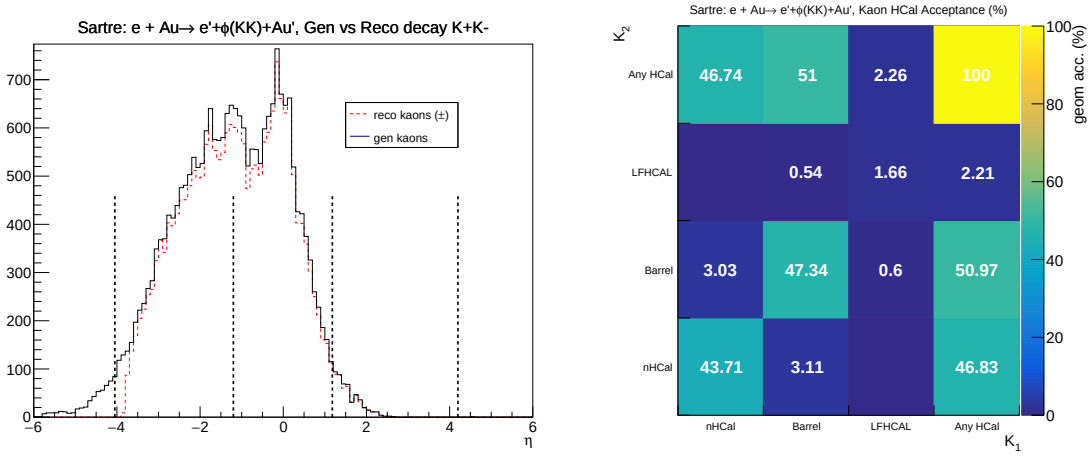

Figure 2.8: `sartre` central production $\phi \to K_1 K_2$ diffractively produced in eAu collisions (18x110). Left: x-Bjorken distributions of decay kaons (solid = generated, dashed = reconstructed) with the vertical dashed lines indicating the ePIC HCal acceptances (from left to right: nHCal | Barrel | LFHCAL). Right: fractions in an HCal acceptance of decay kaons. All combinations of ePIC HCals are investigated, as indicated by the matrix. The fraction for (K_1, K_2) to be in any hadronic calorimeter is 100% (numbers in yellow box). The fraction of both LFHCAL and nHCal combinations is 0%. The fractions were obtained by normalizing by the number of events with two kaons reconstructed by the ePIC tracking system (`ReconstructedChargedParticles`).

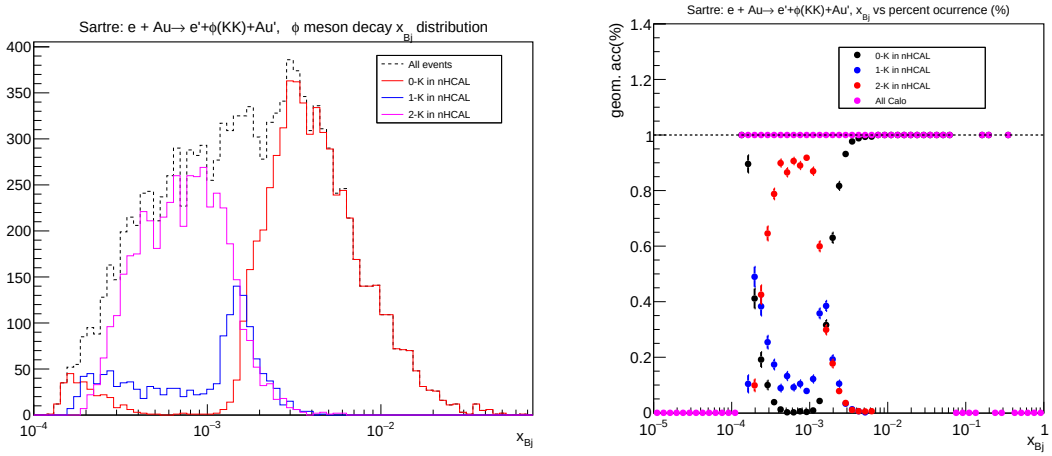

Figure 2.9: `sartre` central production $\phi \to KK$ diffractively produced in eAu collisions (18x110). Left: x-Bjorken distributions of reconstructed decay kaons, split up into the cases of 0, 1, or 2 kaons reconstructed in the nHCal. Right: decay kaon fractions for the three different cases in the nHCal versus x_{Bj}.

3 Summary and next steps

The occurrence of vector mesons and their decay products in the nHCal were studied using generic DIS (`pythia`) and diffractive (`sartre`) event generators. For the studied diffractive events, the nHCal is the only ePIC hadronic calorimeter providing information for a significant (up to 50%) fraction of events with increasing trend for low x-Bjorken, low x-Pomeron, low Q^2, and low values of negative t-Mandelstam. The next steps will be as follows:

3.1 Other diffractive decay channels from central productions

We will study diffractively produced vector mesons decaying into di-leptons and mesons in a systematic way, including but not limited to $J/\psi \to ee$, $J/\psi \to \mu\mu$, $\Upsilon \to ee$, $\Upsilon \to \mu\mu$, $\rho^0 \to \pi^+\pi^-$, and $\phi \to K^0_L K^0_S$, which will likely require making requests to the central production team.

3.2 Cluster level information and nHCal geometry

In addition to track level, we plan to study cluster-level information to confirm actual deposits of decay products in the nHCal. This analysis step will require implementing track(-segment)-to-cluster matching. This approach also offers the possibility to modify the nHCal geometry to study possible design alternatives such as varying tile sizes or a KLM-type design.

3.3 Towards a realistic-type analysis

The current analysis of decay products is tailored to study the coverage of nHCal acceptance in dependence on the process. The analyzed data sets as well as the analysis technique are not realistic in the sense that in real ePIC data, there will for example not only be one exclusive ϕ-meson per event; there will be huge semi-inclusive DIS and combinatorial background as well. Furthermore, it goes without saying that in a real-data analysis, it will not be possible to tag decays on generator level and then navigate to the reconstructed level. There will be tracks, calorimeter clusters, and PID information to work with.

We will implement such type of analysis in close collaboration with the WGs (exclusive, etc). One has to decide what type of questions one wants to answer with which type of study. To justify the physics case for the nHCal, it is important to know what fraction of events would be lost or could not be analyzed in full depth in the absence of the nHCal. This question can well be answered by dedicated diffractive productions. It is then up to a physics-type analysis to study how well the overall ePIC detector and its reconstruction methods can actually tag the events of interest in future experimental data. One first step will be to identify the method of creating a realistic DIS sample that contains diffractive processes, possibly by embedding `sartre` events into `pythia`. We will check with the exclusive WG whether such or a similarly suitable ePIC event sample exists already.

In identifying exclusive meson decays, there will be a loop over all tracks and a discriminator between leptons and hadrons will be needed. A cut on reconstructed track multiplicity will likely be beneficial. Hadrons will be grouped together and pairs with opposite charge will be used to calculate an invariant mass, which can then be used to cut in a window around the PDG parent meson mass. At this step, one has to assign a daughter mass hypothesis, with possible wrong assignments. Exclusive events can be identified with a missing-mass/-energy technique, or kinematic event fitting, if all particles

have been reconstructed. It will have to be checked whether this approach yields good enough information without using hadron (RICH) PID, or whether this information has to be added. For meson decays like $\phi \to K^+K^-$ or $K^0_S \to \pi^+\pi^-$, one can also use a cut on the two-dimensional Armenteros representation to cleanly select kaons or pions.

This document is doi:10.5281/zenodo.14200156.

Appendix A ePIC simulations 101

The centrally produced simulations are analyzed following the instructions on the ePIC software tutorial website [8] linked from the ePIC landing page [9]. Day-to-day updates are communicated on the ePIC Mattermost channels [10]. Caroline (CR) works on BNL's SDDC using an EIC computing account and with `eic-shell` set up. The undergraduate students Dhruv (DS) and Roland (RN) work on their personal laptops with root installations and use input simulated data transferred by CR with `sftp` from SDCC. Access to the simulation files on SDCC is done via

```
mc ls S3/eictest/EPIC/RECO/path-to-directory
```

Runlists are created via (the following 3 lines are *one command* without line break)

```
mc find S3/eictest/EPIC/RECO/path-to-directory --name "*hiDiv_1*.root" |

   sed "s|S3/eictest/||g"  |

   sed 's|^|s3https://eics3.sdcc.bnl.gov:9000/eictest/|g'  > runlist.txt
```

where the host address `s3https://eics3.sdcc.bnl.gov:9000/` allows you to stream the data from the original location without having to copy it to your local area. To that end, it is necessary to first export keys and configure the host as follows:

```
export S3_ACCESS_KEY=ask_on_Mattermost

export S3_SECRET_KEY=ask_on_Mattermost

mc config host add S3 https://eics3.sdcc.bnl.gov:9000 $S3_ACCESS_KEY $S3_SECRET_KEY
```

The `RECO` directories in the path names above contain the reconstructed, i.e., tracked, particles after the primary generated particles have been sent through a `GEANT4` model of the ePIC detector.

- The `MCParticles` branch stores the generated particles after `GEANT`.
- The `ReconstructedChargedParticles` branch stores the reconstructed charged particles.
- The `ReconstructedChargedParticleAssociations` branch provides the link between the two, i.e., for a given reconstructed particle we can navigate back to the generated particle, and for a generated particle we can check if it was reconstructed.
- The `_MCParticles_parents` and `_MCParticles_daugthers` branches provide indices and counters to navigate between decay parent and daughter.

An example printout from a `pythia` event is shown in Fig. A.1, displaying all 26 particles generated in that event.

CR uses two `root` macros [11], which are executed one after the other and which were further developed by DS and RN. The analysis macro produces `root` histograms in one output file, which is read by the plotting macro to produce plots with kinematic distributions. The main frame of the analysis macro is a loop over the generated particles in `MCParticles`.

- Only `MCParticles.generatorStatus` 1 (stable) or 2 (decay particle) are considered; 4 is beam particle, and a two-digit generator status is related to di-quarks.
- Meson decays are tagged and counted on event level by checking their PDG particle type, `MCParticles.PDG`, and that of their daughters. The PDGs of their daughters are counted. Parent and daughter kinematics are stored in histograms.
- The number of all generated particles is counted and some kinematic histograms are filled.
- Lastly, for each generated particle, the matching reconstructed charged particle is found in a loop over the generated $\leftrightarrow$ reconstructed associations, i.e., a loop over the reconstructed particles. Based on the active event decay tags, counts of reconstructed decay particles are incremented and some kinematic histograms are filled.

Global fractions are calculated at the end of the analysis macro. It is important to note that this analysis currently considers only reconstructed secondary decay particles a) from that can be navigated back to the parent, and b) that has a matching generated particle. Naturally this neglects SIDIS and combinatorial background one would have in a real experiment when reconstructing an invariant or missing mass.

The particle counts from analyzing 100 `pythia` neutral current (NC) (18x275) minQ2=1 files in `S3/eictest/EPIC/RECO/24.07.0/epic_craterlake/DIS/NC/5x41/minQ2=1` are summarized in Fig. A.2. Eta distributions produced by the plotting macro for the same data set are shown in Fig. A.3. One notices that the scattered electron is typically in the backward (negative rapidity) and the beam or produced hadrons tend to be in the forward (positive rapidity). As demonstrated in Fig. A.4, higher combinations of beam energies boost the produced particles to higher absolute values of rapidity. Higher and highest Q^2 squeeze the particles towards the barrel, as shown in Fig. A.5.

With separate `root` macros adapted from the module *Analysis and working with the simulation output* [8], tracking efficiencies and resolutions were determined. Examples are shown in Fig. A.6 for a `pythia` NC (5x41) minQ2=1 simulation.

```
Ev#: 581, P-index: 0, PDG: 2212, GenStatus:4, i_parents: 0, i_daughters: 2, pb: 0, pe: 0, db: 1, de: 2
Ev#: 581, P-index: 1, PDG: 2, GenStatus:61, i_parents: 1, i_daughters: 1, pb: 0, pe: 0, db: 5, de: 5
Ev#: 581, P-index: 2, PDG: 2101, GenStatus:63, i_parents: 1, i_daughters: 5, pb: 0, pe: 3, db: 8, de: 12
Ev#: 581, P-index: 3, PDG: 11, GenStatus:4, i_parents: 0, i_daughters: 1, pb: 3, pe: 3, db: 4, de: 4
Ev#: 581, P-index: 4, PDG: 11, GenStatus:21, i_parents: 1, i_daughters: 2, pb: 3, pe: 1, db: 6, de: 13
Ev#: 581, P-index: 5, PDG: 2, GenStatus:21, i_parents: 1, i_daughters: 2, pb: 1, pe: 4, db: 6, de: 13
Ev#: 581, P-index: 6, PDG: 2, GenStatus:23, i_parents: 2, i_daughters: 1, pb: 4, pe: 6, db: 7, de: 7
Ev#: 581, P-index: 7, PDG: 2, GenStatus:62, i_parents: 1, i_daughters: 5, pb: 6, pe: 2, db: 8, de: 12
Ev#: 581, P-index: 8, PDG: 221, GenStatus:2, i_parents: 2, i_daughters: 3, pb: 2, pe: 2, db: 14, de: 16
Ev#: 581, P-index: 9, PDG: 111, GenStatus:2, i_parents: 2, i_daughters: 2, pb: 2, pe: 2, db: 17, de: 18
Ev#: 581, P-index: 10, PDG: 213, GenStatus:2, i_parents: 2, i_daughters: 2, pb: 2, pe: 2, db: 19, de: 20
Ev#: 581, P-index: 11, PDG: 2112, GenStatus:1, i_parents: 2, i_daughters: 0, pb: 2, pe: 2, db: 21, de: 20
Ev#: 581, P-index: 12, PDG: 111, GenStatus:2, i_parents: 2, i_daughters: 2, pb: 2, pe: 4, db: 21, de: 22
Ev#: 581, P-index: 13, PDG: 11, GenStatus:1, i_parents: 2, i_daughters: 0, pb: 4, pe: 8, db: 23, de: 22
Ev#: 581, P-index: 14, PDG: 211, GenStatus:1, i_parents: 1, i_daughters: 0, pb: 8, pe: 8, db: 23, de: 22
Ev#: 581, P-index: 15, PDG: 211, GenStatus:1, i_parents: 1, i_daughters: 0, pb: 8, pe: 8, db: 23, de: 22
Ev#: 581, P-index: 16, PDG: 111, GenStatus:2, i_parents: 1, i_daughters: 2, pb: 8, pe: 9, db: 23, de: 24
Ev#: 581, P-index: 17, PDG: 22, GenStatus:1, i_parents: 1, i_daughters: 0, pb: 9, pe: 9, db: 25, de: 24
Ev#: 581, P-index: 18, PDG: 22, GenStatus:1, i_parents: 1, i_daughters: 0, pb: 9, pe: 10, db: 25, de: 24
Ev#: 581, P-index: 19, PDG: 211, GenStatus:1, i_parents: 1, i_daughters: 0, pb: 10, pe: 10, db: 25, de: 24
Ev#: 581, P-index: 20, PDG: 111, GenStatus:2, i_parents: 1, i_daughters: 2, pb: 10, pe: 12, db: 25, de: 26
Ev#: 581, P-index: 21, PDG: 22, GenStatus:1, i_parents: 1, i_daughters: 0, pb: 12, pe: 12, db: 24, de: 26
Ev#: 581, P-index: 22, PDG: 22, GenStatus:1, i_parents: 1, i_daughters: 0, pb: 12, pe: 16, db: 24, de: 26
Ev#: 581, P-index: 23, PDG: 22, GenStatus:1, i_parents: 1, i_daughters: 0, pb: 16, pe: 16, db: 24, de: 26
Ev#: 581, P-index: 24, PDG: 22, GenStatus:1, i_parents: 1, i_daughters: 0, pb: 16, pe: 20, db: 24, de: 26
Ev#: 581, P-index: 25, PDG: 22, GenStatus:1, i_parents: 1, i_daughters: 0, pb: 20, pe: 20, db: 24, de: 26
Ev#: 581, P-index: 26, PDG: 22, GenStatus:1, i_parents: 1, i_daughters: 0, pb: 20, pe: 16, db: 24, de: 26

decay (GenStatus = 2): η→π⁺π⁻π⁰   stable particle (GenStatus = 1): π±, photon; no daughters
pythia8NCDIS_18x275_minQ2=1_beamEffects_xAngle=-0.025_hiDiv_1.0998.eicrecon.tree.edm4eic   beam particle (GenStatus = 4): proton, electron; no parents
```

Figure A.1: List of particles and some of their properties for one `pythia` NC (18x275) minQ2=1 event. Column 2 is the particle index. Column 3 is the PDG particle type. Column 4 the generator status. Column 5 (6) the number of parents (daughters). Stable particles have no daughters. Beam particles have no parent. Daughter particles from the same decay are grouped together. Column 7 (8) is the particle index (column 2) of the first (last) parent, and similarly for the daughters in column 9 (10). In this example, particle #8 is an η-meson (PDG 221, generator status 2) that decays into two charged pions (PDG 211, considered stable in this simulation) and one neutral pion (PDG 111), which decays into two photons (PDG 22), here particles #23 (db = "daughters begin" = 23) and #24 (de = "daughters end" = 24).

"pythia8NCDIS_18x275_minQ2=1_beamEffects_xAngle=-0.025_hiDiv_1_100files"

```
Number of generated events: 57723

Number of generated electrons +-: 63255
Number of generated protons +-: 53062
Number of generated muons +-: 456
Number of generated pions +-: 342238
Number of generated pi0: 196594, of which decay into 2 gamma: 194251
Number of generated kaons +-: 34137
Number of generated rho0: 26779, of which decay into pi+ pi-: 26750, into mu+ mu-: 1, into e+ e-: 3
Number of generated rho+: 48841
Number of generated phi: 1165, of which decay into K+ K-: 579
Number of generated omega: 26341
Number of generated J/Psi: 0
Number of generated Upsilon: 0
Number of generated D0: 2362
Number of generated B0: 9

Number of reconstructed electrons +-: 59261
Number of reconstructed protons +-: 18568
Number of reconstructed muons +-: 390
Number of reconstructed pions +-: 210930
Number of reconstructed kaons +-: 21775
```

Figure A.2: Particle counts from a `pythia` NC (18x275) minQ2=1 simulation.

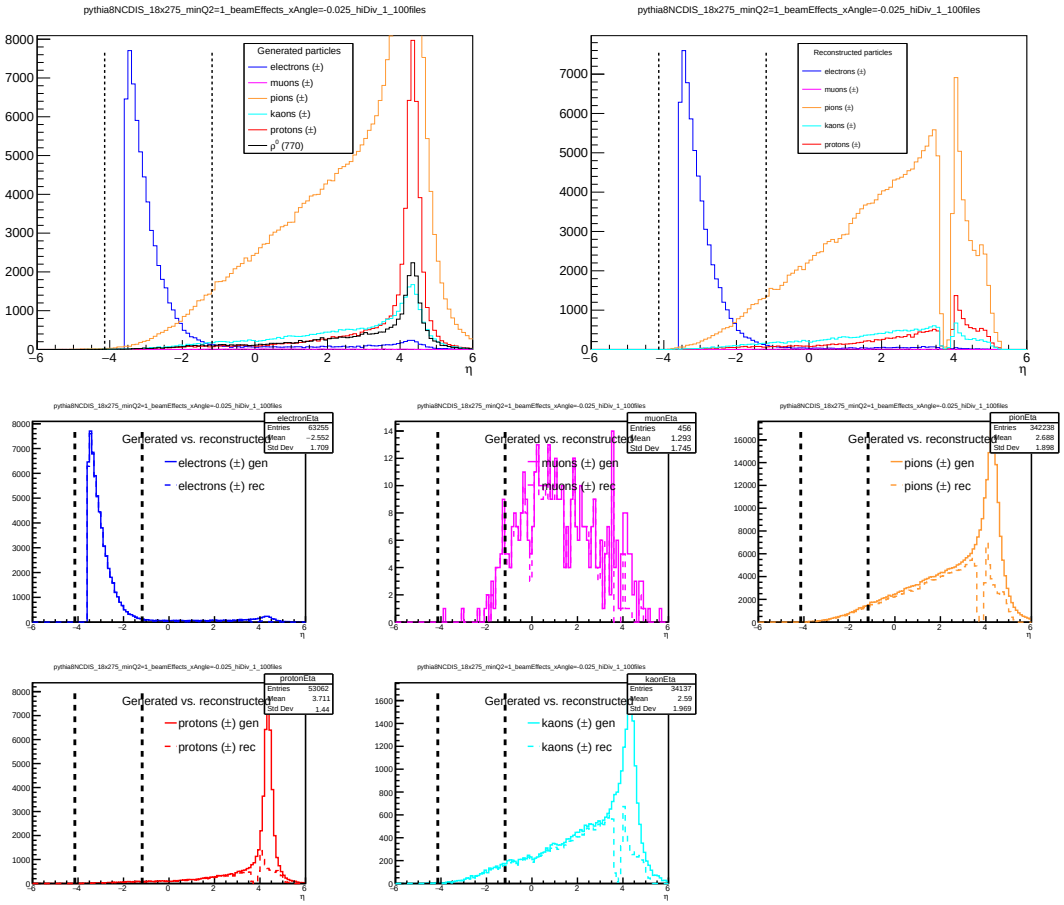

Figure A.3: Particle distributions from a `pythia` NC (18x275) minQ2=1 simulation. Top: particles combined in the same panel and distinguished by color, but separately for generated (left) and reconstructed (right). Middle and bottom: particles separately but showing generated (solid) and reconstructed (dashed) distributions separately. The integrated counts for this data sets are listed in Fig. A.2. The dip in the reconstructed distribution at around $\eta = 4$ indicates where the main ePIC tracking acceptance ends and where then B0 reconstruction sets in at higher positive rapidity. The dashed vertical lines indicate the acceptance of the nHCal.

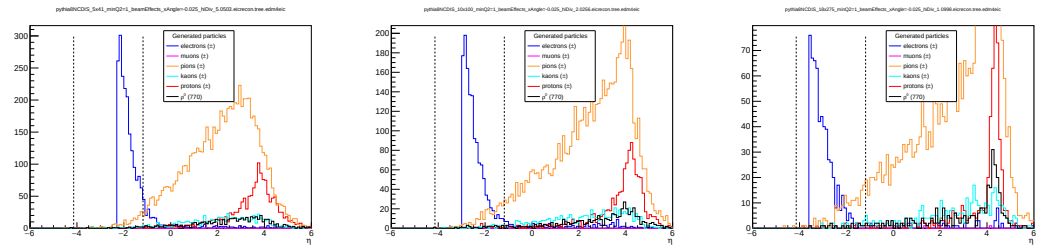

Figure A.4: Generated particle distributions from `pythia` NC minQ2=1 simulation for different beam energies. Left: (5x41); middle: (10x100); right: (18x275).

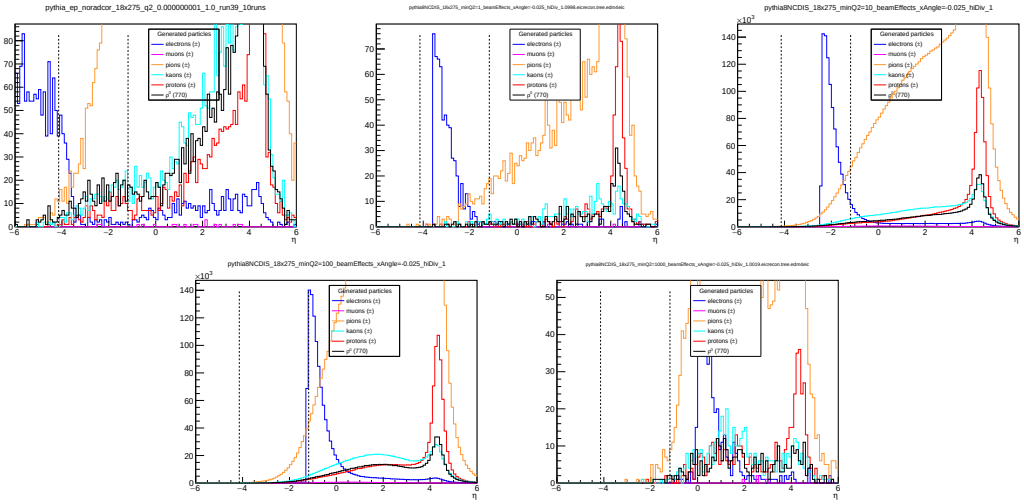

Figure A.5: Generated particle distributions from `pythia` NC (18x275) simulation for different minimum Q^2/GeV^2. Top left: photoproduction ~ 0; top middle: 1; top right: 10; bottom left: 100; bottom right: 1000.

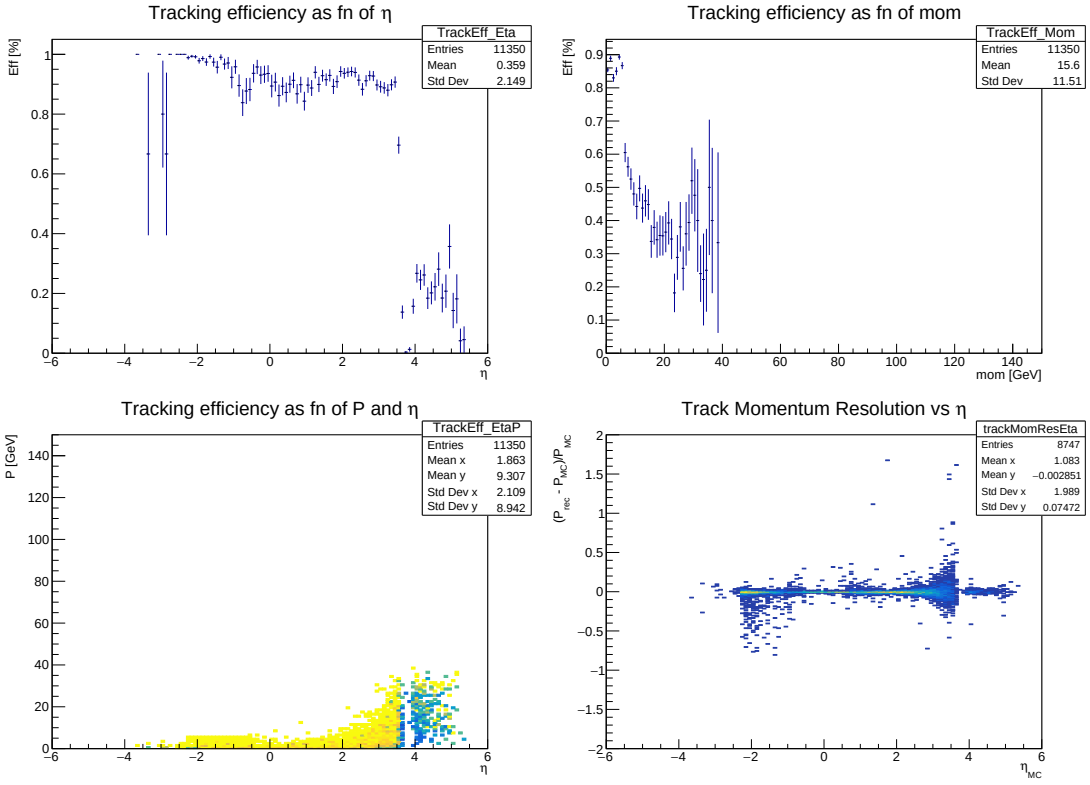

Figure A.6: Tracking efficiency and momentum resolution for `pythia` NC (5x41) minQ2=1. Top left: tracking efficiency vs. rapidity; top right: tracking efficiency vs. momentum; bottom left: tracking efficiency vs. rapidity and momentum; bottom right: momentum resolution vs. rapidity.

List of Tables

List of Figures

References

[1] R. Abdul Khalek, A. Accardi, J. Adam et al., *Science Requirements and Detector Concepts for the Electron-Ion Collider: EIC Yellow Report*, Nucl. Phys. A **1026** (2022) 122447, doi:10.1016/j.nuclphysa.2022.122447.

[2] S. J. Brodsky, V. E. Lyubovitskij, I. Schmidt, *The diffractive contribution to deep inelastic lepton-proton scattering: Implications for QCD momentum sum rules and parton distributions*, Phys. Lett. B **824** (2022) 136801,doi:10.1016/j.physletb.2021.136801.

[3] ZEUS collaboration, *Measurement of the cross-section ratio $\sigma_{\psi(2S)}/\sigma_{J/\psi(1S)}$ in exclusive photoproduction at HERA* J. High Energ. Phys. **2022**, 164 (2022), doi:10.1007/JHEP12(2022)164.

[4] C. Riedl, Status of simulation studies for the nHCal, presentation at the nHCal DSC meeting, September 20, 2024.

[5] V. Andrieux, Fraction of muons from diffractive VM production inside nHCAL, presentation at the nHCal DSC meeting, August 23, 2024.

[6] L. Kosarzewski, Backward Hadronic Calorimeter for ePIC, presentation at the ePIC collaboration meeting, July 25, 2024.

[7] D. Sharma, R. Nothnagel, Phi Meson Decay & Kaon Detection in the nHCal, presentation at the nHCal DSC meeting, November 20, 2024.

[8] ePIC software and analysis tutorials, https://eic.github.io/documentation/tutorials.html, accessed November 14, 2024.

[9] ePIC landing page, https://eic.github.io/documentation/landingpage.html, accessed November 14, 2024.

[10] ePIC Mattermost, https://chat.epic-eic.org/, accessed November 14, 2024.

[11] C. Riedl's github repository for nHCal vector-meson analysis, https://github.com/criedl77/nHCal_VM, accessed November 15, 2024.